International Conference on Applied Energy 2020
Dec. 1 - Dec. 10, 2020, Bangkok / Virtual
Paper ID: 163

The impact of micro-porous layer penetrating into gas diffusion layer on the performance of proton exchange membrane fuel cells

Xiaoqing Zhang, Jiapei Yang, Xiao Ma*, Shijin Shuai

State Key Laboratory of Automotive Safety and Energy, School of Vehicle and Mobility, Tsinghua University, Beijing, 100084, China

E-mail: max@tsinghua.edu.cn

ABSTRACT

The structure and properties of gas diffusion layer (GDL) and micro-porous layer (MPL) are crucially important for the performance of proton exchange membrane fuel cells (PEMFCs). Among which, the penetration of MPL into GDL is a common and critical phenomenon. However, the related research is still insufficient. In order to investigate the impact of MPL penetrating into GDL on fuel cells performance, a three-dimensional multiphase model is described, and the impact of different penetration rate and inlet relative humidity (RH) are discussed. The results demonstrate that larger penetration rate causes better performance due to the better water management. Besides, the liquid water accumulates in the transition region, which increases the oxygen transport resistance.

Keywords: PEMFCs, GDL, MPL, penetration, water management

NONMENCLATURE

Abbreviations	
BP	bipolar plate
CH	flow channel
CL	catalyst layer
GDL	gas diffusion layer
MEM	membrane
MPL	micro-porous layer
TR	transition region
Symbols	
ε	porosity
θ	contact angle
κ	conductivity

1. INTRODUCTION

PEMFCs are one of the promising vehicle power sources owing to its high efficiency, low to zero emission and quick cold start [1]. Typically, PEMFCs consist bipolar plate (BP), flow field, GDL, MPL, catalyst layer (CL) and membrane (MEM). Among PEMFCs, GDL and MPL are important transportation channels for reactant and liquid water. And they have significant impact on water management and performance of fuel cells [2]. Oh et al. [3] utilized the pore size gradient in GDL to improve the fuel cells water management and found that this structure could enhance the bending stiffness of GDL. The perforation is another method to modify the GDL, which results in a better water balance, especially in dry conditions [4]. Besides, Zhou et al. [5] found that MPL improves the fuel cells ohmic transport and performance stability, and the thermal conductivity is the most important parameter.

Due to the materials and preparation process, the MPL made of carbon particle, usually penetrates into the GDL made of carbon fiber, and form a transition region (TR) [6]. Compared to the GDL and MPL, the TR has unique characteristics, including porosity, pore size distribution, permeability, and wettability and so on, which influences the fuel cells water and heat management and performance. Cho et al. [7] prepared the GDL and MPL with different penetration thickness and found that the large penetration thickness is beneficial to improve the fuel cells transient response and balance the capillary pressure gradient, however, the carbon corrosion is also prone to occur in TR. Based on the results of high-resolution neutron imaging, Preston et al. [8] pointed out that there is a region with gradual property changes between GDL and MPL, and proposed a model to describe this phenomenon. Moreover, Wong et al. [9] investigated the impact of MPL penetration on the oxygen transport in GDL under different saturated conditions, the results demonstrated that a deeply intruded MPL leads to lower breakthrough saturation and higher oxygen diffusion performance, especially under high saturated condition.

Although extensive and in-depth researches on GDL and MPL have already been conducted, the literature usually regards these as two separated layers [10, 11]. The study on the penetration of MPL into GDL is still really insufficient, especially the systematic study based on mathematical model. Hence, in this paper, a fuel cells model considering the TR between GDL and MPL is described to investigate the effect of TR thickness on water management and performance of fuel cells under different inlet RH. Furthermore, the agglomerate sub-model is also coupled with the fuel cells model to accurate describe the concentration loss in CL.

2. FUEL CELLS MODEL

2.1 Conversion equations

The fuel cells computational domain is shown in Fig 1, and the assumptions of the model are listed as follows: the fuel cells operate at steady state; all the gas species are ideal gas; the gas and liquid two phase flow are laminar; the MPL and CL are homogeneous and isotropic, while the TR is considered spatial variable properties and the GDL is considered anisotropic; the water produced in CL is in liquid form [12].

The governing equations utilized in this model are listed as follows.

Mass of gas mixture:

$$\nabla\cdot\left(\rho_{\mathrm{g}}\vec{u}_{\mathrm{g}}\right)=S_{\mathrm{m}} \tag{1}$$

Momentum of gas mixture:

$$\nabla\cdot\left(\frac{\rho_{\mathrm{g}}\vec{u}_{\mathrm{g}}\vec{u}_{\mathrm{g}}}{\varepsilon^{2}\left(1-s\right)^{2}}\right)=-\nabla P_{\mathrm{g}} +\mu_{\mathrm{g}}\nabla\cdot\left(\nabla\left(\frac{\vec{u}_{\mathrm{g}}}{\varepsilon\left(1-s\right)}\right)+\nabla\left(\frac{\vec{u}_{\mathrm{g}}}{\varepsilon\left(1-s\right)}\right)^{\mathrm{T}}\right) -\frac{2}{3}\mu_{\mathrm{g}}\nabla\cdot\left(\nabla\left(\frac{\vec{u}_{\mathrm{g}}}{\varepsilon\left(1-s\right)}\right)\right)+S_{\mathrm{u}} \tag{2}$$

Gas species:

$$\nabla\cdot\left(\rho_{\mathrm{g}}\vec{u}_{\mathrm{g}}Y_{\mathrm{i}}\right)=\nabla\cdot\left(\rho_{\mathrm{g}}D_{\mathrm{eff}}^{\mathrm{i}}\nabla Y_{\mathrm{i}}\right)+S_{\mathrm{i}} \tag{3}$$

Energy:

$$\nabla\cdot\left(\varepsilon s\rho_{\mathrm{l}}C_{\mathrm{p,l}}\vec{u}_{\mathrm{l}}T+\varepsilon\left(1-s\right)\rho_{\mathrm{g}}C_{\mathrm{p,g}}\vec{u}_{\mathrm{g}}T\right)= \nabla\cdot\left(k^{\mathrm{eff}}\nabla T\right)+S_{\mathrm{T}} \tag{4}$$

Liquid water in channel:

$$\nabla\cdot\left(\rho_{\mathrm{l}}\vec{u}_{\mathrm{l}}s\right)=S_{\mathrm{l}} \tag{5}$$

Liquid water in porous media (GDL, TR, MPL and CL):

$$0=\nabla\cdot\left(\rho_{\mathrm{l}}\frac{Kk_{\mathrm{l}}}{\mu_{\mathrm{l}}}\nabla P_{\mathrm{l}}\right)+S_{\mathrm{l}} \tag{6}$$

Dissolved water:

$$\nabla\cdot\left(\frac{n_{\mathrm{d}}}{F}I_{\mathrm{ion}}\right)=\frac{\rho_{\mathrm{MEM}}}{EW}\nabla\cdot\left(D_{\mathrm{d}}^{\mathrm{eff}}\nabla\lambda\right)+S_{\mathrm{mw}} \tag{7}$$

Electronic charge:

$$0=\nabla\cdot\left(k_{\mathrm{e}}^{\mathrm{eff}}\nabla\varphi_{\mathrm{e}}\right)+S_{\mathrm{e}} \tag{8}$$

Ionic charge:

$$0=\nabla\cdot\left(k_{\mathrm{ion}}^{\mathrm{eff}}\nabla\varphi_{\mathrm{ion}}\right)+S_{\mathrm{ion}} \tag{9}$$

In this study, the porosity distribution in TR is considered linearly decreases from GDL to MPL, and the permeability is calculated by the Kozeny-Carman relation [13]:

$$K=\frac{\varepsilon^{3}d^{2}}{16k_{\mathrm{k}}\left(1-\varepsilon\right)^{2}} \tag{10}$$

The benchmark parameters used in the Kozeny-Carman relation is ε=0.4 and K=2*10^{-13}. Other parameters used in the model are listed in Table 1.

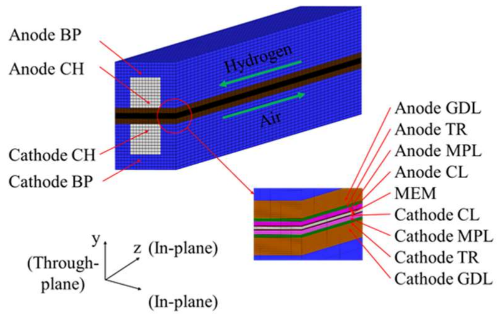

Fig 1 Computational geometry and mesh

Table 1 Physical properties and operating conditions

Parameters	Values
Channel length (mm)	50
Channel width (mm)	1
Channel height (mm)	1
Land width (mm)	1
BP height (mm)	0.5
Thickness (mm) (MPL, CL, MEM)	0.04, 0.01, 0.0254

Total thickness of GDL and TR (mm)	0.2
Contact angle (°) (GDL, TR, MPL, CL)	135, 110, 105, 100
Intrinsic permeability (m^2) (GDL, MPL, CL, MEM)	4.0×10^{-12}, 2.0×10^{-13}, 1.0×10^{-13}, 2.0×10^{-20}
Porosity (GDL, MPL)	0.7, 0.4
Stoichiometric ratio	Anode: 2.0, Cathode: 2.5
Reference current density (A m^{-2})	16000
Operating pressure (atm)	1.5
Operating temperature (K)	353.15
Agglomerate radius (m)	5.0×10^{-7}
Electrolyte film thickness (m)	5.0×10^{-8}

2.2 Boundary conditions

The inlet and outlet boundary conditions are mass flux and pressure, respectively. The temperature in all walls are fixed at 353.15K, and the electronic charge is defined as $\varphi_{\mathrm{ele}}^{\mathrm{a}}=E_{\mathrm{rev}}-V_{\mathrm{out}}$ and $\varphi_{\mathrm{ele}}^{\mathrm{c}}=0$ at the anode and cathode terminals.

3. RESULT AND DISCUSSION

3.1 Model validation

In order to validate the accuracy of the model, the polar curves under different inlet RH are simulated and compared with the experimental data [14] as shown in Fig 2. The parameters used in simulation are same with the experiment, and the results indicate that the simulation results are agreeable well with the experiment.

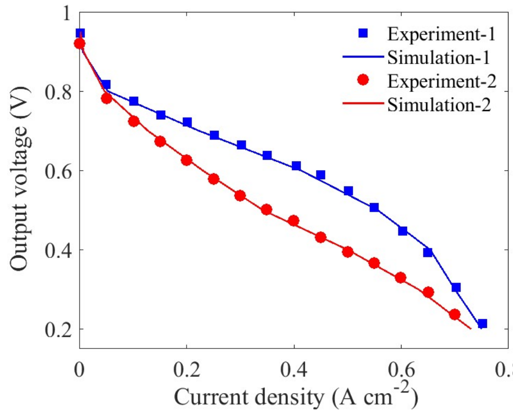

Fig 2 Comparison of polar curve with experimental data

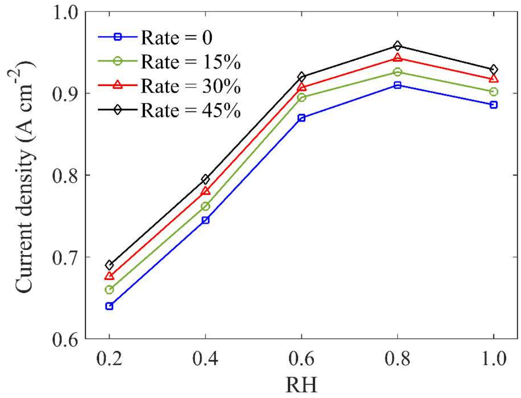

(a)

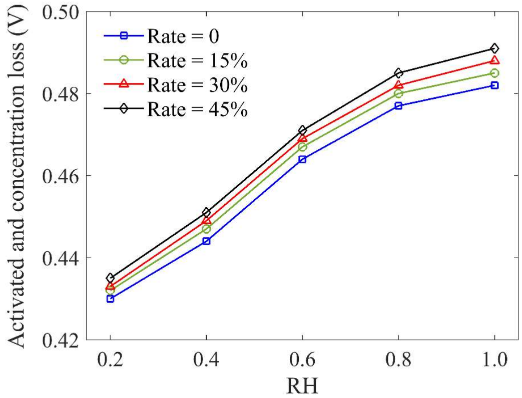

(b)

Fig 3 Effect of penetration rate and inlet RH on fuel cells performance (a) and activated and concentration loss (b)

3.2 Fuel cells performance

The MPL penetration changes the properties of GDL and form a TR. Because the total thickness of GDL and TR is constant, hence, the penetration rate is utilized to present the thickness of GDL and TR. For instance, 15% penetration rate means the GDL thickness is 170μm and the TR thickness is 30μm. As shown in Fig 3(a), the fuel cells with larger penetration rate show better performance, and this conclusion is consistent with the experimental results of Cho et al. [7]. Specifically, when the RH is 1.0, the current density of the fuel cells with the penetration rate of 45% is 1.3%, 3.0% and 4.9% higher than the cases with the penetration rate of 30%, 15% and 0, respectively. Besides, in this research, the best inlet RH is about 0.8, taking the cases with the penetration rate of 45% as an example, compared with the RH of 1.0, 0.6, 0.4 and 0.2, the current density at RH of 0.8 is 3.1%, 4.1%, 20.5% and 38.8% higher, respectively. And this phenomenon does not change with the penetration rate, which means the water and reactant gas transportation are in balance under this RH. When the RH is lower than 0.8, the fuel cells performance also decreases with the decrease of RH, and this is mainly related to the increment of ohmic loss is larger than the decrement of concertation loss. Fig 3(b) shows the quantizing of the activated and concentration loss, and the results demonstrate that the larger penetration rate causes larger activated and concentration loss, and this loss also increases with the increase of RH, which mainly connected with the increase of liquid water. For instance, compared with the cases under the RH of 0.2, the activated and concentration loss of the cases under the RH of 1.0 increases about 12% for all penetration rates. In summary, for fuel cells with different penetration rate, the balance between the oxygen transport resistance and ohmic resistance is the key factor affecting the fuel cells performance, and in this research, the oxygen transport resistance is affected by the depth of TR and the liquid water distribution, and the ohmic resistance is affected by membrane water content. Hence, the water management, including liquid water and membrane water management, will be analyzed carefully in the next two sections.

3.3 Liquid water management

Liquid water could change the oxygen transport path and affect the membrane water content. Fig 4 shows the liquid water distribution under the inlet RH is 1.0 and 0.2. The results demonstrate that the liquid water accumulates in the TR, and the saturation decreases from the GDL side to MPL side, which is agreeable with the experimental conclusions based on the synchrotron X-ray radiography [15, 16] and neutron imaging [8]. This phenomenon also indicates that the conventional fuel cells model, which usually ignores the TR between GDL and MPL, might underestimate the liquid water saturation in this region. Besides, for the fuel cells operating at high inlet RH, the liquid water saturation in GDL are basically the same for fuel cells with different penetration rate, considering the fuel cells with large penetration rate, the current density and liquid water production is high, which indicates that large penetration rate could enhance the drainage capacity of GDL. Furthermore, when the fuel cells operate under low inlet RH, the higher liquid water saturation in MPL and CL is conducive to increase membrane water content and decrease the ohmic resistance. It should be noted that, with the increasing of penetration rate, the peak of liquid water profile in TR gradually get away from the CL, and the peak value decreases with the increase of penetration rate. Specifically, when the RH is 0.2, as the penetration rate increases from 15% to 45%, the peak values are 0.191, 0.181 and 0.170, respectively. In a nutshell, TR could utilize the capillary force gradient to speed up GDL drainage under high RH, while it could prevent membrane dehydration under the low RH and improve fuel cells performance.

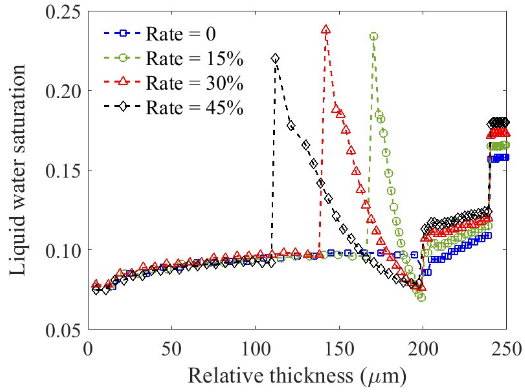

(a)

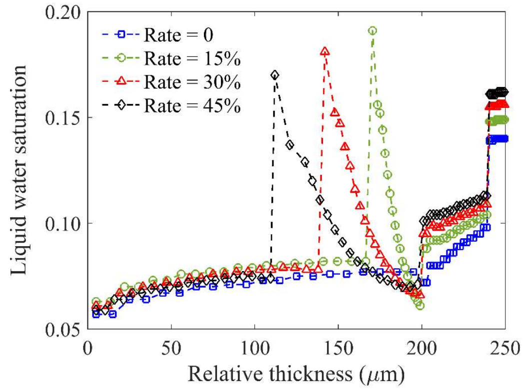

(b)

Fig 4 Effect of penetration rate on liquid water distribution under the inlet RH is 1.0 (a) and 0.2 (b)

3.4 Membrane water management

Membrane water content could affect the ionic conductivity. As shown in Fig 5, when the inlet RH is 0.4 and 0.6, the fuel cells with large penetration rate have higher average membrane water content in membrane electrode assembly (MEA), and the largest difference is 12.1%. The membrane water content under other inlet RH is very close for different penetration rate. However, the membrane water content distribution is different for the fuel cells with different penetration rate, taking Fig 6 as an example, when the inlet RH is 1.0, the membrane water content in cathode CL increases with the increase of penetration rate, especially in the region under channel, and the same is true for electrochemical reaction rate. This phenomenon demonstrates that for the fuel cells with large penetration rate, there is large current density in the region with small ohmic resistance, and this is conducive to reduce the ohmic loss.

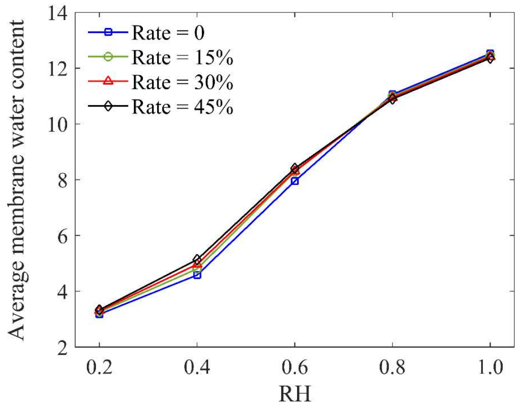

Fig 5 Effect of penetration rate and inlet RH on volume average membrane water content of MEA

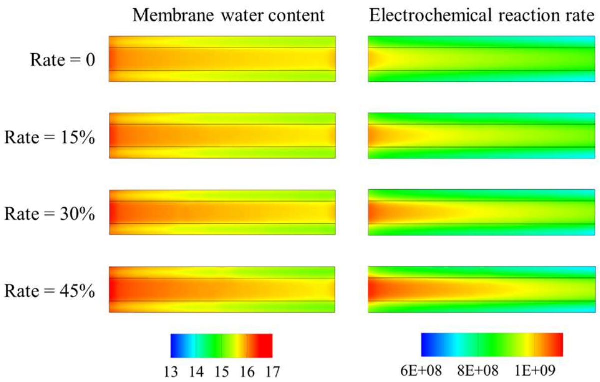

Fig 6 Membrane water content (left) and electrochemical reaction rate (right) in the middle of cathode CL under the inlet RH is 1.0

4. CONCLUSION

In this paper, a three-dimensional multiphase non-isothermal fuel cells model is described, in which the agglomerate sub-model and the TR between the GDL and MPL are coupled. And the impact of MPL penetrating into GDL on the performance under different inlet RH are investigated. The results demonstrate that larger penetration rate causes better performance. Besides, there is liquid water accumulation in the TR, and the peak of liquid water saturation in GDL and TR moves to channel side with the increase of penetration rate. Moreover, the penetration of MPL could improve the water management by enhancing the capillary force and the membrane water content.

ACKNOWLEDGEMENT

This research is supported by the Beijing Municipal Science & Technology Commission (Grant No. Z181100004518004), National Key R&D Program of China (Grant No. 2018YFB0105403) and National Key R&D Program of China “Integration and Control of Fuel Cell Engine for Heavy Duty Truck & Assessment Technologies of Fuel Cell Engine Reliability for Heavy Duty Truck”.

REFERENCE

[1] Ren P, Pei P, Li Y, Wu Z, Chen D, Huang S. Degradation mechanisms of proton exchange membrane fuel cell under typical automotive operating conditions. Prog Energy Combust Sci 2020;80:100859.

[2] Wong AKC, Ge N, Shrestha P, Liu H, Fahy K, Bazylak A. Polytetrafluoroethylene content in standalone microporous layers: Tradeoff between membrane hydration and mass transport losses in polymer electrolyte membrane fuel cells. Appl Energy 2019;240:549-60.

[3] Oh H, Park J, Min K, Lee E, Jyoung J-Y. Effects of pore size gradient in the substrate of a gas diffusion layer on the performance of a proton exchange membrane fuel cell. Appl Energy 2015;149:186-93.

[4] Alink R, Haußmann J, Markötter H, Schwager M, Manke I, Gerteisen D. The influence of porous transport layer modifications on the water management in polymer electrolyte membrane fuel cells. J Power Sources 2013;233:358-68.

[5] Zhou J, Shukla S, Putz A, Secanell M. Analysis of the role of the microporous layer in improving polymer electrolyte fuel cell performance. Electrochim Acta 2018;268:366-82.

[6] Ozden A, Shahgaldi S, Li X, Hamdullahpur F. A review of gas diffusion layers for proton exchange membrane fuel cells—With a focus on characteristics, characterization techniques, materials and designs. Prog Energy Combust Sci 2019;74:50-102.

[7] Cho J, Park J, Oh H, Min K, Lee E, Jyoung J-Y. Analysis of the transient response and durability characteristics of a proton exchange membrane fuel cell with different micro-porous layer penetration thicknesses. Appl Energy 2013;111:300-9.

[8] Preston JS, Fu RS, Pasaogullari U, Hussey DS, Jacobson DL. Consideration of the Role of Micro-Porous Layer on Liquid Water Distribution in Polymer Electrolyte Fuel Cells. J Electrochem Soc 2011;158:B239-B46.

[9] Wong AKC, Banerjee R, Bazylak A. Tuning MPL Intrusion to Increase Oxygen Transport in Dry and Partially Saturated Polymer Electrolyte Membrane Fuel Cell Gas Diffusion Layers. J Electrochem Soc 2019;166:F3009-F19.

[10] Chen G, Zhang G, Guo L, Liu H. Systematic study on the functions and mechanisms of micro porous layer on water transport in proton exchange membrane fuel cells. Int J Hydrogen Energ 2016;41:5063-73.

[11] Kang K, Ju H. Numerical modeling and analysis of micro-porous layer effects in polymer electrolyte fuel cells. J Power Sources 2009;194:763-73.

[12] Li W, Zhang Q, Wang C, Yan X, Shen S, Xia G, et al. Experimental and numerical analysis of a three-dimensional flow field for PEMFCs. Appl Energy 2017;195:278-88.

[13] Pasaogullari U, Wang C-Y. Two-phase transport and the role of micro-porous layer in polymer electrolyte fuel cells. Electrochim Acta 2004;49:4359-69.
[14] Yan Q, Toghiani H, Causey H. Steady state and dynamic performance of proton exchange membrane fuel cells (PEMFCs) under various operating conditions and load changes. J Power Sources 2006;161:492-502.
[15] Lee J, Chevalier S, Banerjee R, Antonacci P, Ge N, Yip R, et al. Investigating the effects of gas diffusion layer substrate thickness on polymer electrolyte membrane fuel cell performance via synchrotron X-ray radiography. Electrochim Acta 2017;236:161-70.
[16] Lee J, Liu H, George MG, Banerjee R, Ge N, Chevalier S, et al. Microporous layer to carbon fibre substrate interface impact on polymer electrolyte membrane fuel cell performance. J Power Sources 2019;422:113-21.